Available online at www.sciencedirect.com

ScienceDirect

Energy Reports 7 (2021) 657–676

www.elsevier.com/locate/egyr

Tmrees, EURACA, 28 to 30 May 2021, Athens, Greece

Robust space–time modeling of solar photovoltaic deployment

Sergio Copiello*, Carlo Grillenzoni

University IUAV of Venice, Department of Architecture, Dorsoduro 2206, 30123 Venice, Italy

Received 13 July 2021; accepted 27 July 2021

Abstract

Solar photovoltaic (PV) has established itself as a fairly promising, fast-growing renewable energy source. The main determinants of solar PV deployment are thought to be physical and climatic factors – such as latitude and solar irradiance, not to mention terrain and built environment features – as well as socio-economic drivers — such as population density, household size, and education level. Besides, peer effects and neighborhood effects are found to affect the willingness to adopt solar photovoltaic systems strongly. This study aims to set up robust space–time models, which enable us to investigate the drivers of solar PV deployment using fine-grained spatial and temporal data. We use space–time auto-regressive models (STAR) with several exogenous covariates that are expected to explain the installed solar PV capacity. STAR models require the specification of spatial weight matrices (W). As in regular lattice data, we select causal (lower triangular) W matrices so that the consistency of least-squares (LS) estimators is warranted. We show that they can be extended to robust LS estimators, which are necessary because of strong outlier contamination. Models are tested on the Italian municipal data of residential and industrial PV plants installed under the support schemes in force between 2006 and 2011. Empirical results confirm the important role played by the space–time dynamic components. Significant exogenous predictors are found in the domains of the physical features (elevation and land area), demography (population), built environment (residential buildings), and socio-economic aspects (income, employment rate, commuter workers).

Peer-review under responsibility of the scientific committee of the Tmrees, EURACA, 2021.

Keywords: Photovoltaic systems; Renewable energy sources; Socio-economic determinants; Serial and spatial dependence; Robust estimation

1. Introduction

1.1. Solar photovoltaic energy in the framework of the European Green Deal

Between late 2019 and early 2020, the European Commission has put forward the European Green Deal (from now on, EGD), a new action plan meant to protect the health and safeguard the well-being of citizens [33] by enhancing the sustainability of the Union's economic system [29]. The EGD has been conceived in a landscape dominated by massive concerns for the effects exerted by human activities on the climate and the environment

* Corresponding author.
E-mail address: sergio.copiello@iuav.it (S. Copiello).

https://doi.org/10.1016/j.egyr.2021.07.087

Peer-review under responsibility of the scientific committee of the Tmrees, EURACA, 2021.

Nomenclature

Elv	Elevation (m.)
Csr	Commuter students (pct. of commuter students in the population)
Cwr	Commuter workers (pct. of commuter workers in the population)
Emr	Employment rate (ratio between employed people and the total population)
Flu	Firms' local units (unit-to-population ratio)
Her	Higher-education rate (pct. of graduates in the population)
i, j	indexes of time and space lags
Inc	Disposable income per capita (Euros)
l, m	Index and number of exogenous regressors
Lat	Latitude (deg.)
n, T	Number of spatial units and number of time periods
N	Number of observations (sample size)
Pop	Population (inhab.)
R06	Share of residential buildings built after 2006 (pct.)
R81	Share of residential buildings built after 1981 (pct.)
Rbd	Residential buildings (building-to-population ratio)
s, t	Space and time indexes
Ser	Secondary-education rate (pct. of people with a secondary school diploma)
Lan	Land area (km2)
Unr	Unemployment rate (ratio between unemployed people and the total labor force)
W	Spatial weights matrix
X	Matrix of exogenous regressors
y	Dependent variable
y_{oa}	Installed photovoltaic capacity (kW), overall
y_{norm}	Installed photovoltaic capacity (kW), normalized by population

[18,28,73]. The ambitious long-term goals of the EGD are as follows: to cut down to zero the net emissions of greenhouse gases by 2050 – namely, climate neutrality – and to decouple the economic growth from resource use [29]. The EGD is built upon several pillars, which involve changes in the energy, manufacturing, building, and transportation industries. For instance, industrial sectors are required to mobilize towards a climate-neutral and circular economy, while the construction sector is asked to double – at least – the renovation rate of the building stock [60].

As far as energy generation, supply, and use are concerned, the keyword is decarbonization. The clean energy transition implies quick phasing out of coal, plus an additional effort to decarbonize natural gas. Furthermore, the EGD envisages that the power sector should become primarily based on renewable energy sources. Under this framework, it can be easily understood that the further development of solar photovoltaic (PV) power generation is bound to be a cornerstone [36,37]. The growth in the use of renewable energy sources has been widely documented over the last years [16,34,37], and this especially holds for PV. In the last ten years or so, PV capacity has more than doubled or tripled in Germany, Italy, and several other countries, although the growth was much stronger in the first half of the decade. The whole European Union has increased its cumulative PV capacity by a factor of four over the same time span [37]. Similar trends are experienced elsewhere [35,70].

1.2. Economic drivers for the uptake of solar photovoltaic energy

Although the cost–benefit balance of solar PV systems has been questioned in the past, recent studies highlight both the economic viability and the environmental sustainability of this option depending on a range of climate and market conditions [27,56,75]. Technological development aside [23], the financial feasibility is boosted by the sharp reduction in the cost of PV modules, namely, a steady downward trend over the last four decades [40,51]. The upfront costs of PV systems are expected to further decline in the short to mid-term, which should offset the decline in public funding [15] and make this source cost-competitive to others [72]. However, economic viability is not the only explanation for the quick uptake of PV. We are currently facing a growing corpus of studies focusing on the determinants of solar PV deployment, which range from physical and climatic factors to socio-economic drivers [2]. Furthermore, spatial interactions, especially in the form of peer effects and neighborhood effects, are found to play a remarkable role [5]. This implies that considering the spread of PV systems simultaneously over time and across space is an essential step to draw a comprehensive picture of the phenomenon.

1.3. Aim and structure of the study

Here we aim to investigate solar PV deployment drivers by dealing with fine-grained spatial and temporal data. To that end, this study adds to the recent literature by setting up various space–time models and searching for robust estimates, which is both methodologically and computationally challenging [9]. The models are tested on the installed PV capacity in more than seven thousand Italian municipalities between 2006 and 2011. The remainder of this paper is arranged as follows. The next section briefly summarizes the known determinants of PV deployment as found in the recent literature. Section 3 is devoted to presenting the method and the models. Section 4 introduces the case study and describes the solar PV deployment data analyzed here. Section 5 discusses the results. Lastly, Section 6 draws the conclusions.

2. Literature review

According to the literature published in the last decade, the determinants of PV deployment can be clustered into three groups: physical and climatic factors are included in the first set, socio-economic variables are the focus of the second group, spatial interactions – such as peer effects, neighborhood effects, and spatial spillovers – shape the third cluster.

As far as physical and climatic factors are concerned, solar irradiance and latitude are often called forth first. They are controlled for in the analytical models of several studies and found to be significant predictors of PV deployment [5,6,44,66,69], along with terrain surface features and local climate conditions [69]. Similarly, the characteristics of the built environment - e.g., housing density, proximity to urban settlements, the share of detached houses, age of the housing stock — are found to play a role in affecting the uptake of PV installations [5,6,20,21,30,43,58,66,68].

Incentive policies and subsidies aside [49,58], among the socio-economic determinants of PV deployment are demographic aspects such as household size and population density, as well as social features like the share of owner-occupied homes and the education level [5,8,20,21,43,47,48,66]. The role of disposable income is debated [6] since it is often found to exert a positive influence [5,20,21,65,66], while sometimes it negatively affects the use of renewable energy sources [8,9,14] or it is weakly related to them [30]. Besides, concerns about rising oil and electricity prices push the adoption of PV systems [10,26,30,44,48]. A systematic and comprehensive literature review on socio-economic predictors driving residential solar PV adoption has recently been published [2].

A prolific research strand has focused on the possibility that PV deployment is also driven by peer and neighborhood effects [17]. By this it is meant that the attitude to adopt innovations in general, and specifically solar PV systems, is partly shaped by the emulation of mainstream behavior or the willingness to stick to social norms [19]. Those who see friends, colleagues, or neighbors [9,50] adopting PV systems are more willing to adopt the same systems for themselves too. The same expectation holds for any other kind of group that could trigger social interaction [53]. Hence, an individual is more likely to adopt PV systems if a large portion of his social reference group does it [39], which gives rise to spatial diffusion patterns [30] when social groups are spatially clustered. The occurrence of peer and neighborhood effects has been studied using a variety of methods and models: survey-based analyses [1,42,49,57,62,76,77]; agent-based models [59,63]; epidemic diffusion models [64]; econometric approaches especially based on spatial autoregressive models and spatial panel models with fixed or random effects [3,5,21,30,43,47,48,66]; geographically weighted regression models [6]. All the above-referenced works agree in identifying spatial interactions as a key driver to explain the adoption and diffusion of PV systems. Notably, the potential occurrence of spatial spillovers is indirectly suggested by specific socio-economic predictors, such as in the case of the positive relationship between the adoption of PV systems and the population that commutes over half an hour to work [9].

3. Method and models

3.1. Space–time models

Let $\{y_{st}\}$ be a dataset of photovoltaic power system installations, measured on n areal units for T periods; more precisely, $s = 1, 2 \dots n$ is the spatial index of sites (municipalities), $t = 1, 2 \dots T$ is the time index of periods (years) and $N = n \times T$ is the total sample size. Also, let us consider a set of time-invariant explanatory variables $\{x_{ls}\}$, where $l = 1, 2 \dots m$ is the index of covariates (both physical and socio-economic). The mathematical model which may represent such data is the Space–Time AutoRegression with eXogenous variables (STARX); assuming *first order* dynamics and a single regressor ($m = 1$), the model is given by:

$$y_{st} = \alpha + \varphi_1 y_{s,t-1} + \varphi_2 y_{s-1,t} + \varphi_3 y_{s-1,t-1} + \beta_1 x_s + \beta_2 x_{s-1} + e_{st}, \quad e_{st} \sim \mathrm{IN}(0, \sigma_e^2), \tag{1}$$

where e_{st} are Independent Normal (IN) residuals and $\alpha, \varphi_i, \beta_j, \sigma$ are fixed coefficients. Basically, the solar PV power installed on each s-th site depends on its previous temporal value $y_{s,t-1}$, on its contemporaneous nearest neighbor (NN) $y_{s-1,t}$, on its time lagged NN term $y_{s-1,t-1}$ and on the exogenous regressors and their NN values x_{s-1}. The time-variability can be extended to exogenous variables as x_{lst}; however, major physical covariates (as latitude and altitude) are time-invariant and socio-economic covariates (as population density and housing stock) are nearly so in the medium term, or they may be measured on a census (decadal) basis only.

By extending the space–time dynamics to orders $p, q > 1$, and considering m time-varying regressors, the model of Eq. (1) can be written in its general STARX$_m$(q,p) form as follows:

$$y_{st} = \alpha_0 + \sum_{j=0}^{q}\sum_{i=1}^{p} \varphi_{ji}\, y_{s-j,t-i} + \sum_{l=1}^{m}\sum_{j=0}^{q}\sum_{i=0}^{p} \beta_{lji}\, x_{l,s-j,t-i} + e_{st}, \quad e_{st} \sim \mathrm{IN}(0, \sigma_e^2), \tag{2}$$

This representation encompasses various classes of models, such as the dynamic panel [25, p. 96] if one includes a time-invariant *latent* component $+\delta z_s$ that represents the peculiarities of spatial units. It is worth mentioning that the NN relationship can be extended to encompass k-nearest neighbors (k-NN). However, the strength of the spatial relationship is expected to fade as the distance increases (Fig. 1), in accordance with the so-called Tobler's first law of geography: "everything is related to everything else, but near things are more related than distant things" [71, p. 236]. Also, by dropping the third sum (in i) in the Eq. (2), one has an extension of the model of Eq. (1) to multiple regressors.

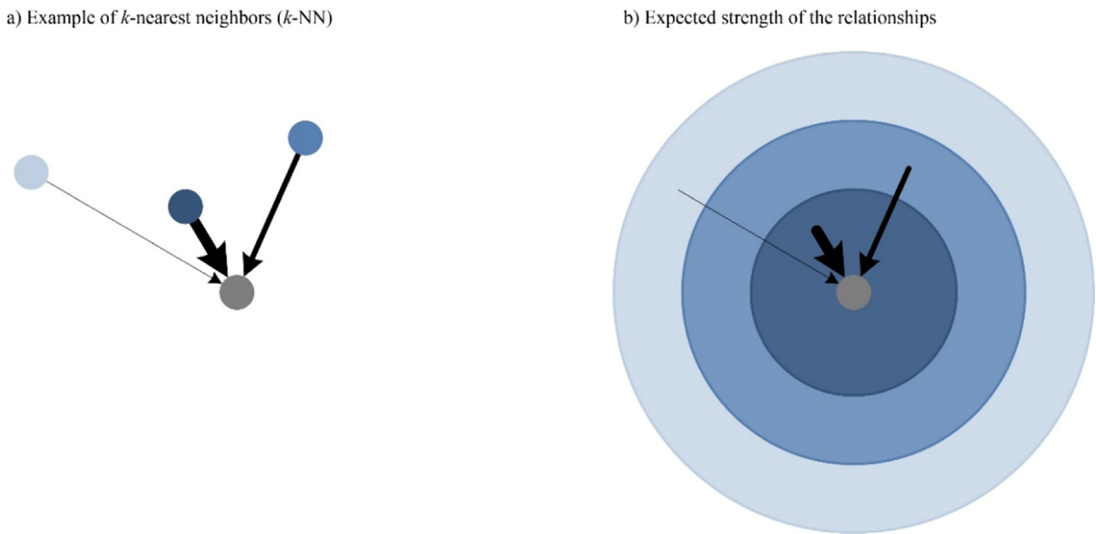

Fig. 1. Example of k-NN with $k = 3$ (a): distance and expected strength of the spatial relationships (b).

The primary characteristic of the model in Eq. (2) is the STAR component of the first double summation. This component is useful in forecasting [31] and must be properly designed; however, in the study of the PV determinants the unbiased estimation of coefficients β_{lji} is the major concern for energy policy decisions. It is known that in the presence of autocorrelation of errors e_{st} the parameter estimates are not efficient, and their standard errors are not consistent [4], so that the statistical inference on the models is biased. Once again, the dynamic structure of Eq. (2) must be properly designed, both at temporal and spatial level, to generate uncorrelated residuals.

A related statistical issue arises from the spatial *location* of the NN or k-NN terms $y_{s-j,t-i}$. If they are unrestricted (at 360 degrees), then the "regressors" $y_{s-j,t-i}$ in the model of Eq. (2) may be correlated with the errors e_{st}, making the estimates of β_{lji} also biased (see Appendix). In general, the identification of causal dynamics is much more challenging across space than in time. This is because relationships over time are unidirectional (from the past to the present, and from the present to the future), while relationships across space are not (from a space unit to another space unit, and vice versa). The issue is more severe than the omission of terms $y_{s-j,t-i}$, and gives rise to several estimation problems in the solar PV field too [9]. It deserves mentioning that those problems fuel "the skepticism exhibited by some authors with respect to the claim of early studies of neighborhood effects" and that "caution is due to methodological challenges in estimation. In some cases, statistical problems invalidate the results". [22, p. 540]. The issue must be solved by properly constraining the adjacent NN or k-NN terms to a specific *one-quadrant* direction, e.g. to the northwest (NW). The (k-)nearest northwestern neighbor(s) NNWN (k-NNWN) constraint (Fig. 2 is consistent with the unidirectional (past–present) dynamics of the temporal component, where $y_{\cdot t-i}$ and $e_{\cdot t}$ are uncorrelated. Also, it is similar to the *identifiability* constraints of classical econometric models, which allows the consistency of parameter estimates [4].

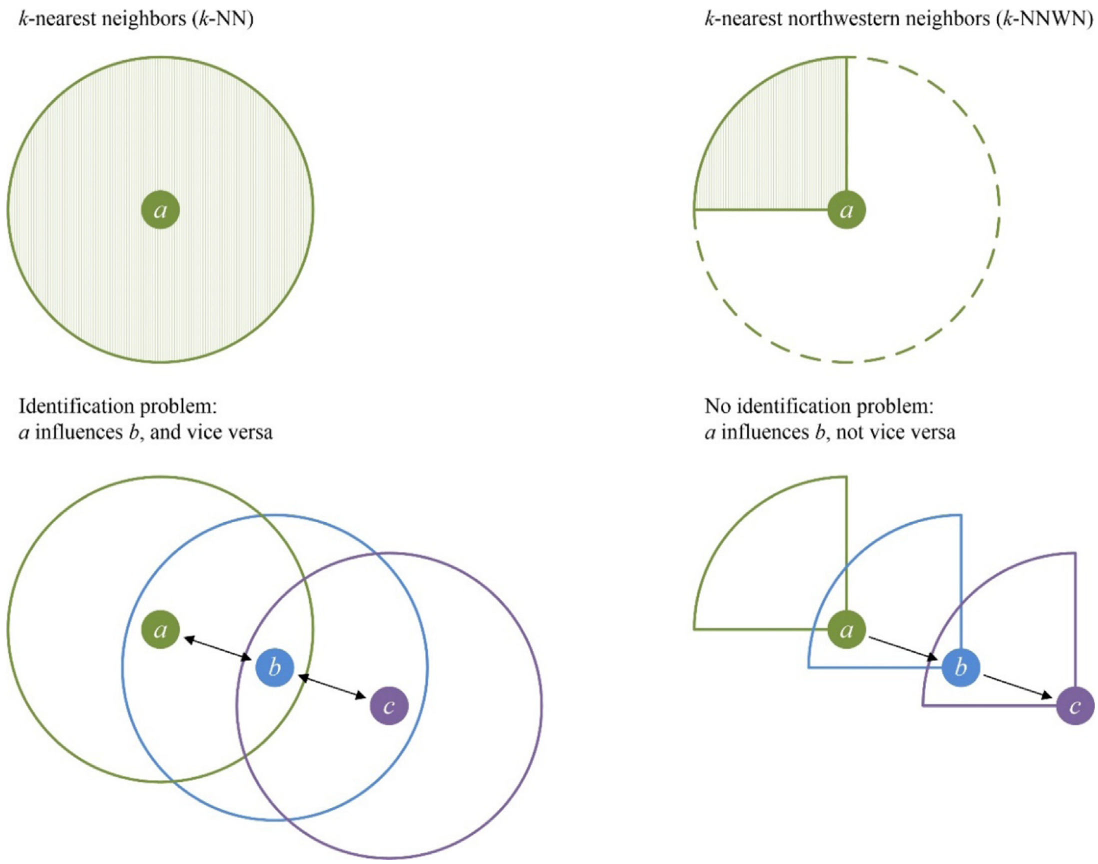

Fig. 2. The (k-)nearest northwestern neighbor(s) NNWN (k-NNWN) constraint.

To further explain the issue, let us use a vector notation by arranging the model components as $\boldsymbol{y}_t = [y_{1t} \dots y_{st} \dots y_{nt}]'$, $\boldsymbol{X}_t = [\boldsymbol{x}_{1t} \dots \boldsymbol{x}_{lt} \dots \boldsymbol{x}_{mt}]$ the matrix of regressors with columns $\boldsymbol{x}_{lt} = [x_{l1t} \dots x_{lst} \dots x_{lnt}]'$, and $\boldsymbol{e}_t = [e_{1t} \dots e_{st} \dots e_{nt}]'$. Following Elhorst [25], the model of Eq. (2) with $p = 1, q = 1$ can be written in matrix form as follows:

$$\boldsymbol{y}_t = \alpha \mathbf{1}_n + \varphi_1 \boldsymbol{y}_{t-1} + \varphi_2 \boldsymbol{W} \boldsymbol{y}_t + \varphi_3 \boldsymbol{W} \boldsymbol{y}_{t-1} + \boldsymbol{X}_t \boldsymbol{\beta}_1 + \boldsymbol{W} \boldsymbol{X}_t \boldsymbol{\beta}_2 + \boldsymbol{e}_t, \quad \boldsymbol{e}_t \sim \mathrm{IN}(\mathbf{0}, \boldsymbol{I}_n \sigma_e^2), \tag{3}$$

where $\mathbf{1}_n$ is a unit vector of length n, $\boldsymbol{\beta}_1 = [\beta_{11} \dots \beta_{1l} \dots \beta_{1m}]'$ and $\boldsymbol{\beta}_2 = [\beta_{21} \dots \beta_{2l} \dots \beta_{2m}]'$ are the coefficients, and $\boldsymbol{W}$ is a $n \times n$ *contiguity* matrix, whose rows $\boldsymbol{w}_s$ have 1 in the positions where the s-th unit is adjacent to others and 0 elsewhere. Model (3) becomes a *panel* data system by adding the *latent* components $(\boldsymbol{u} + v_t \mathbf{1}_n)$ of spatial and temporal, fixed or random effects, which characterize the specific pattern of each unit. The estimation of these components requires a state–space formulation or the inclusion of dummy variables for each unit; however, in the model of Eq. (3) we assume that data matrix $\boldsymbol{X}_t$ includes major local factors and thus we avoid treating it *also* as a panel. Further, in the econometric literature the residual $\boldsymbol{e}_t$ is sometimes assumed as spatially correlated as $\boldsymbol{e}_t = \theta \boldsymbol{W} \boldsymbol{e}_t + \boldsymbol{v}_t$; this condition involves nonlinear estimators and can be avoided by introducing in Eq. (3) the second-order AR term $\varphi_4 \boldsymbol{W}_2 \boldsymbol{y}_t$, where $\boldsymbol{W}_2$ is the matrix of second NN contiguity (still in the NW direction).

3.2. Spatial weights matrices

The sparse array $\boldsymbol{W}$ is also called spatial *weights* matrix and its structure is defined by the proximity rule which is adopted, e.g., single or multiple connections and single or multiple directions, etc. The simplest choice is the first NN link, which implies that every row $\boldsymbol{w}_s$ has a single 1; however, from Eq. (3) the component $\boldsymbol{W} \boldsymbol{y}_t$ may become correlated with the residual $\boldsymbol{e}_t$, thus violating a basic assumption of regression models. The consequence is the bias (thus, inconsistency) of common estimators (see Appendix). To solve this drawback, one may constrain the matrix $\boldsymbol{W}$ in a one-quadrant direction (e.g., to northwest, NW), so that each component $y_{s-1,t} = \boldsymbol{w}_s' \boldsymbol{y}_t$ is independent of e_{st} at any t, namely $\mathrm{E}\left(e_{st} | y_{s-1,t}\right) = 0$. Accordingly, every row $\boldsymbol{w}_s$ has a single 1 if and only if the first NN link is placed in the NW quadrant (Fig. 3), thus corresponding to the notion of nearest northwestern neighbor (NNWN). In practice, with the NW constraint, the errors e_{st} are all placed in the south, east and south-east (SE) directions with respect to the observation $y_{s-1,t}$ (see Appendix); notice that this approach may also allow for multiple NN selections, provided they all satisfy the NW constraint.

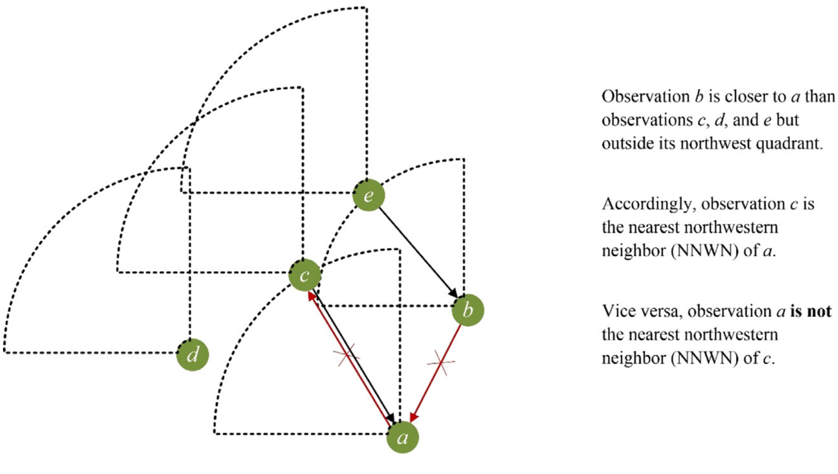

Fig. 3. Constraining the spatial weights matrix to the first nearest northwestern neighbor (NNWN).

The approach of constraining $\boldsymbol{W}$ unidirectionally is typical of lattice data, as digital images y_{ijt} [13,31], where the spatial index s is replaced by the indices *i,j* of row and column. For example, the *westward* lagged model $y_{ijt} = \alpha + \varphi y_{i,j-1,t} + e_{ijt}$ has a matrix $\boldsymbol{W}$ with 1 under the main diagonal and 0 elsewhere. It is statistically identified, because the spatial predictions $\hat{y}_{ij+1t}$ can sequentially be computed from $\hat{y}_{ijt}$ and an initial condition $\hat{y}_0$ on the left border. Instead, the two-sided filter $y_{ijt} = \alpha + \varphi(y_{i,j-1,t} + y_{i,j+1,t})/2 + e_{ijt}$ cannot be used in predictions, as $y_{i,j+1,t}$ is unknown and depends on $e_{i,j+1,t}$. This example can be easily extended to models with time-lagged regressors; it shows that spatial identification of the $\boldsymbol{W}$ matrix is strictly related to the sequential computation of predictions, as in pure time series models.

Under the NW constraint of the $\boldsymbol{W}$ matrix, the OLS estimator of STARX models is consistent (see Appendix). To derive it, we can write the model (3) in vector form as $\boldsymbol{y}_t = \boldsymbol{Z}_t'\boldsymbol{\delta} + \boldsymbol{e}_t$, where $\boldsymbol{\delta}' = \left[\alpha, \varphi_1, \varphi_2, \varphi_3, \boldsymbol{\beta}_1', \boldsymbol{\beta}_2'\right]$ is the vector of parameters and $\boldsymbol{Z}_t = \left[\boldsymbol{1}_n, \boldsymbol{y}_{t-1}, \boldsymbol{W}\boldsymbol{y}_t, \boldsymbol{W}\boldsymbol{y}_{t-1}, \boldsymbol{X}_t, \boldsymbol{W}\boldsymbol{X}_t\right]$ is the matrix of regressors, with spatial and temporal lagged data. Thus, defining the *stacked* data matrix $\boldsymbol{Z}_N = [\boldsymbol{Z}_1; \boldsymbol{Z}_2; \ldots; \boldsymbol{Z}_T]$, with $N = n \cdot T$, one can obtain the OLS estimator of the model (3) as $\hat{\boldsymbol{\delta}}_N = (\boldsymbol{Z}_N'\boldsymbol{Z}_N)^{-1}\boldsymbol{Z}_N'\boldsymbol{y}_N$, where $\boldsymbol{y}_N = \left[\boldsymbol{y}_1; \boldsymbol{y}_2; \ldots; \boldsymbol{y}_T\right]$. As shown in the simulation experiments of Appendix, the matrix $\boldsymbol{W}$ is *triangular* under the one-quadrant contiguity constraint, and it allows $\hat{\boldsymbol{\delta}}_N$ to be consistent with unbiased covariance matrix $\hat{\boldsymbol{\Sigma}}_N = \hat{\sigma}_e^2(\boldsymbol{Z}_N'\boldsymbol{Z}_N)^{-1}$.

In the application to the data of PV deployment, we also estimate the model of Eq. (3) in temporal *local* form, by regressing the ending data $\boldsymbol{y}_T$ on its previous and surrounding values $\boldsymbol{W}\boldsymbol{y}_{T-i}, i > 0$, and on the fixed available regressors. In this case, the model of Eq. (3) becomes:

$$\boldsymbol{y}_T = \alpha_0\boldsymbol{1}_n + \sum_{i=1}^{p}\varphi_{1i}\boldsymbol{y}_{T-i} + \sum_{i=0}^{p}\varphi_{2i}\boldsymbol{W}\boldsymbol{y}_{T-i} + \sum_{l=1}^{m}\beta_{1l}\boldsymbol{x}_{lT} + \sum_{l=1}^{m}\beta_{2l}\boldsymbol{W}\boldsymbol{x}_{lT} + \boldsymbol{e}_T \tag{4}$$

In vector form, the matrix of regressors is given by $\boldsymbol{Z}_n = \left[\boldsymbol{1}_n, \boldsymbol{W}\boldsymbol{y}_T, \boldsymbol{Y}_T, \boldsymbol{W}\boldsymbol{Y}_T, \boldsymbol{X}_T, \boldsymbol{W}\boldsymbol{X}_T\right]$, where $\boldsymbol{Y}_T = [\boldsymbol{y}_{T-1} \ldots \boldsymbol{y}_{T-p}]$, which has n rows; here, the OLS $\hat{\boldsymbol{\delta}}_n$ provides local (at T) estimates on the previous years.

3.3. Robust estimation

The interest in the OLS estimator is motivated by its flexibility and adaptability in the presence of anomalous observations (outliers). These produce significant bias on coefficients; however, OLS method can be made *robust* (resistant) to outliers in a simple way. Since for the model of Eq. (3) it minimizes the sum of squared residuals

$$\hat{\boldsymbol{\delta}}_N = \arg\ \min\sum_{t=1}^{T}(\boldsymbol{y}_t - \boldsymbol{Z}_t'\boldsymbol{\delta})'(\boldsymbol{y}_t - \boldsymbol{Z}_t'\boldsymbol{\delta}) = \arg\ \min\sum_{t=1}^{T}\sum_{s=1}^{n}e_{st}^2(\boldsymbol{\delta})$$

a robust version can be obtained by replacing the quadratic criterion, with a less divergent loss function (Fig. 4). For example, the absolute value $|e_{st}|$ provides the least absolute deviation (LAD) estimates, which are mildly robust. A more robust solution is provided by a function $\rho(\cdot)$ which censors large values outright:

$$\hat{\boldsymbol{\delta}}_{\mathrm{R}} = \arg\ \min\sum_{t=1}^{T}\sum_{s=1}^{n}\rho[e_{st}(\boldsymbol{\delta})], \quad \text{with} \quad \rho(e) = \gamma \quad \text{if} \quad |e| > \gamma. \tag{5}$$

The *threshold* constant $0 < \gamma < \infty$ is selected according to the rate of outlier contamination; in general, it must achieve a compromise between bias and efficiency of estimates. In practice, small values of γ increase the resistance to outliers, and so their unbiasedness, but reduce their efficiency. Unfortunately, there are not automatic rules for selecting γ [32], as the outlier contamination is unknown both in rate and size.

One of the preferred solutions for the ρ-function is the *bisquare* one of W. Tukey [46]:

$$\begin{aligned} \rho(e) &= \{1 - [1 - (e/\gamma)^2]^3\} \cdot \gamma^2/6 \quad &&\text{if } |e/\sigma_e| \le \gamma, \\ &= \gamma^2/6 &&\text{if } |e/\sigma_e| > \gamma, \end{aligned} \tag{6}$$

The function in Eq. (6) is discontinuous at $e = \gamma$, and this requires iterative algorithms for the minimization of Eq. (5), including the mildly robust LAD estimates. Under Gaussian residuals, the design of γ in Eq. (5) which allows 95% relative efficiency with respect to OLS estimates is given by $\gamma = 4.685$; however, smaller values $2 < \gamma < 4$ may be necessary to achieve unbiasedness under heavy outlier contamination (>5%). Robust estimation of the scale parameter σ_e is necessary for running the estimator in Eqs. (5)-(6); it is usually based on the median absolute deviation (MAD):

$$\hat{\sigma}_{\mathrm{MAD}} = \mathrm{median}(|\hat{e}_{st} - \mathrm{median}(\hat{e}_{st})|) \cdot 1.4827, \tag{7}$$

this is robust against anomalous residuals and is consistent for σ_e under Gaussianity of e_{st}. However, MAD of Eq. (7) underestimates σ_e in general conditions, thus its value is replaced by $\hat{\sigma}_{\mathrm{R}}$ which satisfies the first derivative equation $N^{-1}\sum_{t=1}^{T}\sum_{s=1}^{n}\rho'(\hat{e}_{st}/\sigma_e) = 0$ [74].

Robust estimates of σ_e are also necessary for model evaluation, e.g. with the classical index $R^2 = 1 - (\hat{\sigma}_e/\hat{\sigma}_u)^2$, where $\hat{\sigma}_u$ is computed by robust estimation the mean model $y_{st} = \alpha + u_{st}$. However, a R^2_{MAD} index can be directly

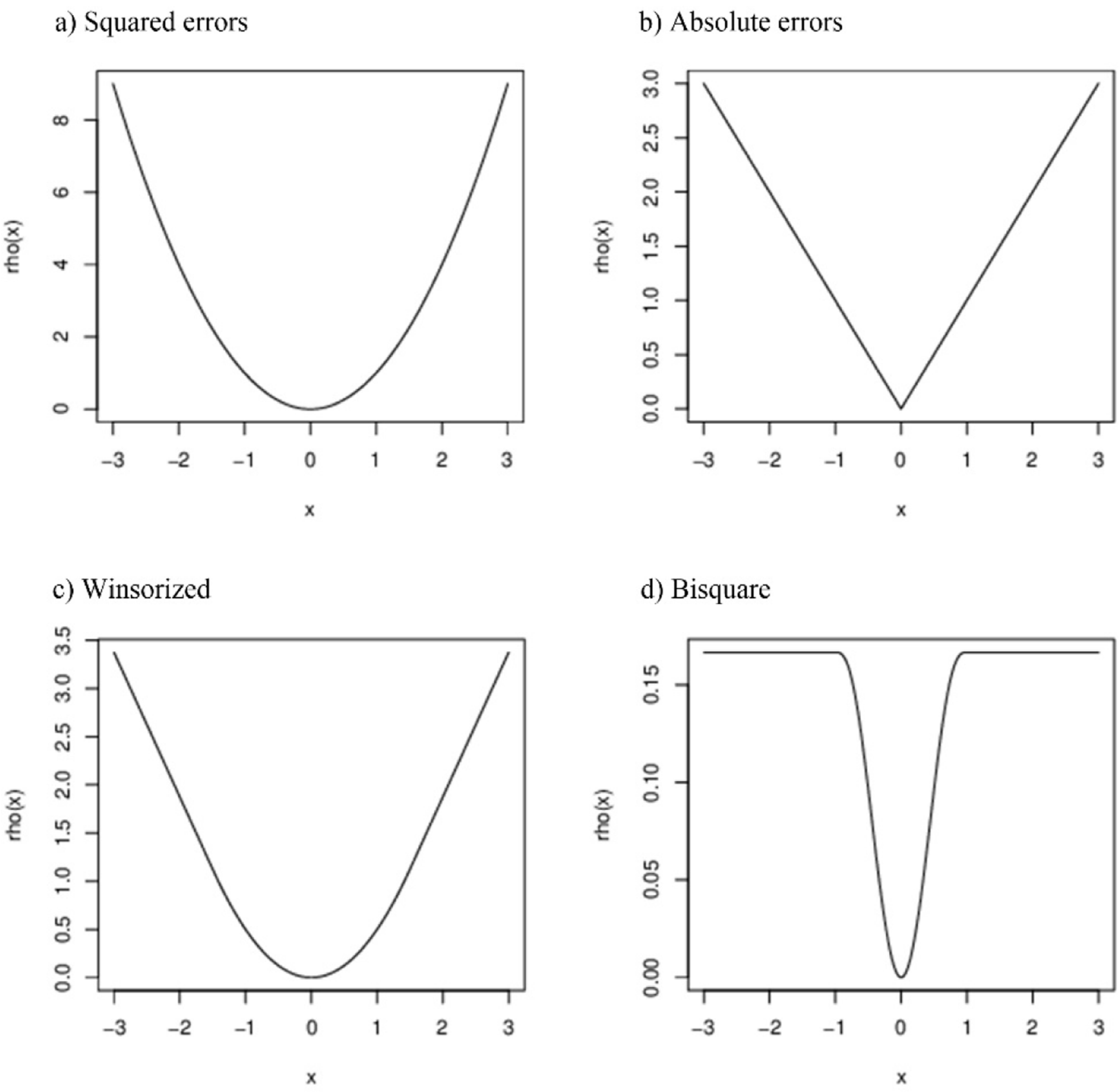

Fig. 4. Estimation functions: (a) Least squares (OLS); (b) Absolute deviations (LAD); (c) Robust winsorized (Huber); (d) Robust bisquare (Tukey).
Source: Bramati [12] and Grillenzoni [32].

computed on the models (3)–(4) as the squared *robust correlation* between $(y_{st}, \hat{y}_{st})$, where $\hat{y}_{st}$ are the fitted values estimated with (5)–(6). A robust correlation coefficient, based on the MAD of standardized variables, is as follows [67]:

$$R_{xy} = \frac{\mathrm{MAD}^2\,(u) - \mathrm{MAD}^2\,(v)}{\mathrm{MAD}^2\,(u) + \mathrm{MAD}^2\,(v)}, \quad \text{with} \quad u, v = \frac{x - \mathrm{E}\,(x)}{\sqrt{2}\mathrm{MAD}\,(x)} \pm \frac{y - \mathrm{E}\,(y)}{\sqrt{2}\mathrm{MAD}\,(y)}. \tag{8}$$

In Appendix, simulation experiments are conducted on contaminated data of the model in Eq. (3); they show that the estimation performance of the method of Eqs. (5)–(6) depends both on the selection of γ and $\boldsymbol{W}$. As in OLS, the one-quadrant specification $\boldsymbol{W}_{\mathrm{NW}}$ provides unbiased estimates, even in the robust estimation.

4. Data

In Italy, the introduction of support schemes for solar PV energy dates back to the early 2000s, with a major revision in 2005. The EU-derived (Directive 2001/77/EC) "Conto energia" program and subsequent adjustments involve a nationwide homogeneous (without regional differences) set of tools, the most important of which are feed-in-tariff and net metering [24,54,61]. The data on all the subsidized photovoltaic plants – both residential and industrial, either building-integrated or ground-mounted – are gathered from the Atlasole geographic information system (now Atlaimpianti[1]), which is managed by GSE Plc, a state-owned company whose mission is to foster and support the use of renewable energy sources in the country.

As far as the time dimension is concerned, we consider the installed photovoltaic capacity between 2006 and 2011, which has been steadily growing (Fig. 5) thanks to the abundant financial support during that time window [11,59]. Even though there have been changes over time, we can essentially consider the program uniform for the purpose of this study. Firstly, the time window we consider mostly overlaps with the first (2005–2006, with installations until 2010) and second (2007–2010) "Conto energia" program, while the two subsequent programs affected the systems put into operation in the first and second half of 2011, respectively. The first program featured a cap on the cumulative installed PV capacity, but the subsequent programs progressively raised it, so the subsidy scheme was renewed. We limit the analysis to 2011 since, around that time, the program has undergone remarkable changes to put a cap on its high costs [59]. Only in mid-2013, thus beyond the time window of this study, the planned cumulative installed PV capacity was reached, and the subsidy scheme discontinued.

As regards the spatial dimension, the observations consist of the installed photovoltaic capacity in 7797 municipalities (LAU level 2 according to the European Local Administrative Units classification). It means that more than 96% of the 8,092 municipalities at the time have at least one subsidized PV plant and, hence, are covered by the analysis. The spatial dependence between the observations is modeled according to the notion of the nearest northwestern neighbor (NNWN), as explained and motivated in the previous section. The excerpt of the map below (Fig. 6) shows the NNWN modeling results on the municipalities located southwest of the city of Venice. Due to the unidirectional relationship starting from the northwest, 27 municipalities placed along the north and northwest borders lack an NNWN, so they are dropped from the analysis. As it can be seen, the NNWN modeling gives rise to a network that consists of multiple threads, which sometimes branch into two or more sub-threads. That means that a parent node – namely, a municipality – can have more than one child node, but a child node has one and only one parent node.

The exogenous variables belong to two main domains: physical conditions and built environment the former, demographic and socio-economic drivers the latter. Physical conditions are described by elevation (*Elv*), latitude (*Lat*), and land area (*Lan*). Both *Lat* and *Elv* are expected to take on a negative sign; this is because the lower the latitude and elevation, the more and larger PV plants we are supposed to find. On the contrary, *Lan* should show a positive sign since the larger a municipality is, the more the PV capacity it can host is. The built environment aspects taken into consideration are as follows: residential buildings (*Rbd*); share of residential buildings built after 2006 (*R06*); percentage of residential buildings built after 1981 (*R81*).

As far as the demographic and socio-economic drivers are concerned, we expect that the variables expressing higher levels of both economic development – employment rate (*Emp*), number of firms' local units normalized by population (*Flu*) – and education – the percentage of people with a secondary school diploma (*Ser*) and the percentage of graduates (*Her*) – are positively correlated with the installed PV capacity. We also include two other predictors about commuting – commuter students (*Csr*) and commuter workers (*Cwr*), both normalized by population – to catch potential spatial spillovers indirectly. Concerning the disposable income per capita (*Inc*), we aim to test whether it is significant or not and the sign it takes on. We consider the installed PV capacity in 2011 as the independent variable both since, shortly after that time, there have been changes in the setting and effectiveness of the support policies [55] and because the demographic and socio-economic predictors refer to the same year. The source for those variables is census data gathered and published by the National Institute of Statistics.

[1] See https://www.gse.it/dati-e-scenari/atlaimpianti (last accessed 29.06.2021).

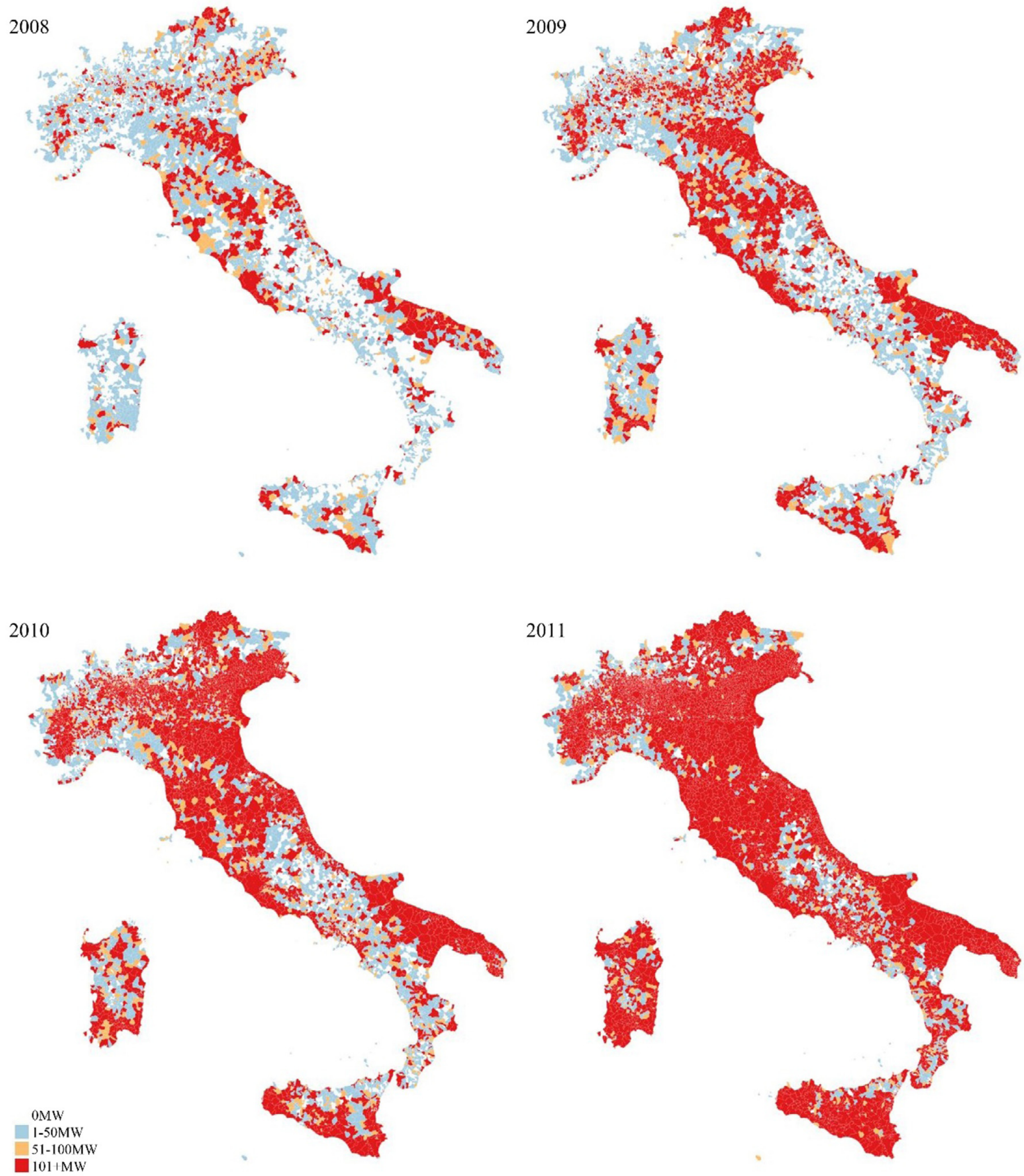

Fig. 5. Cumulative installed capacity in Italian municipalities between 2008 and 2011.

5. Results and discussion

5.1. Results for the local model

The tables below report 95% statistically significant estimates for the *local* model of Eq. (4) concerning total (y_{oa}, Table 1) and normalized by population (y_{norm}, Table 2) installed PV capacity, respectively. We will not bother the reader with the interpretation of the OLS estimates as they are irredeemably flawed, even with heteroskedastic and

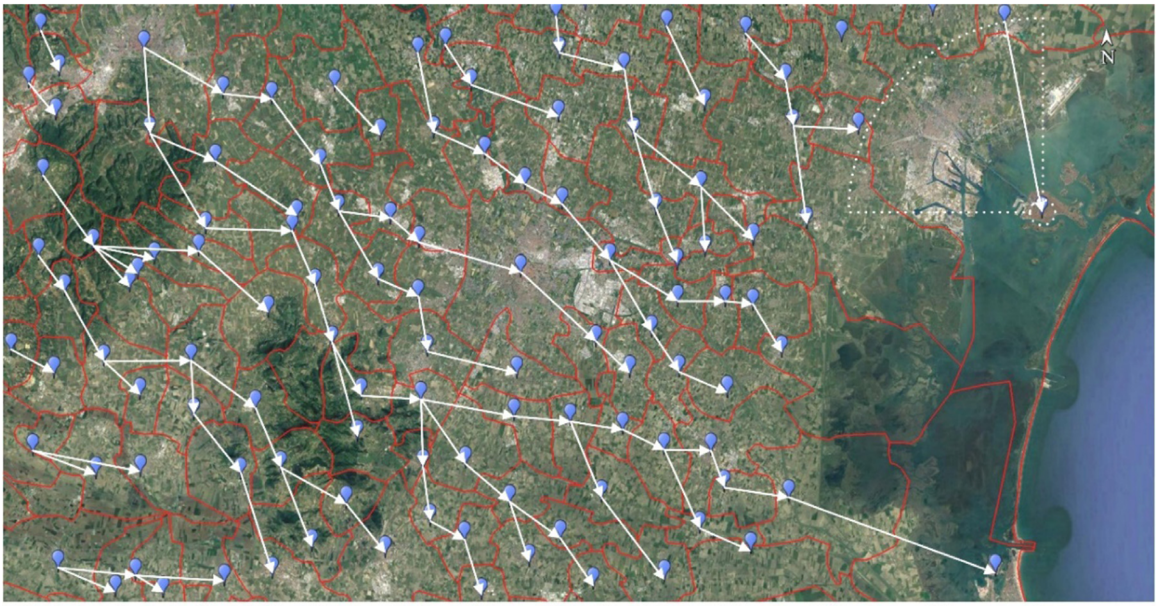

The lower layer is Google Earth's aerial view of the territory Southwest of the city of Venice; red lines are the boundaries of the municipalities; blue icons indicate the administrative centroids of the same municipalities; white arrows represent the spatial dependence relationship.

Fig. 6. Modeling of the spatial dependence relationship according to the notion of the nearest northwestern neighbor (NNWN) *Source:* authors' study based on data from Google Earth and National Institute of Statistics.

Table 1. Parameter estimates of the model in Eq. (4), dependent: y_{oa}, at $t = 2011$ (z_l are t-statistics).

Method	OLS		OLS-HAC		LAD		R-Winsorized		R-Bisquare	
x_l	β_l	z_l	β_l	z_l	β_l	z_l	β_l	z_l	β_l	z_l
Const.	−491.76	−1.799	84.337	0.226	−34.05	−1.713	−87.807	−1.353	−15.259	−0.675
$y_{s,t-1}$	0.5413	23.352	0.7019	3.053	0.9955	5.625	0.9777	158.700	0.9939	341.810
$y_{s,t-2}$	1.1430	14.526			1.1679	3.280	1.0330	49.465	0.6590	66.574
$y_{s,t-3}$	2.8922	14.091	2.8384	2.603	1.7941	5.155	1.4411	26.024	1.4926	56.928
$y_{s,t-4}$							0.6864	4.374	2.8071	38.648
$y_{s,t-5}$	20.101	4.877	22.952	2.328	15.490	2.092	11.514	10.220		
$y_{s-1,t}$	0.0674	7.191	0.0852	3.531			0.0339	13.200		
$y_{s-1,t-1}$	0.0573	2.870			0.0610	2.909	0.0342	5.926		
$y_{s-1,t-2}$					0.2344	3.058	0.1497	7.246	0.0258	3.185
$y_{s-1,t-4}$	−1.2764	−2.140	−1.2086	−2.320						
$y_{s-1,t-5}$							−2.7847	−2.666		
Elv	−1.4502	−11.469	−1.4454	−11.53	−0.1030	−4.310	−0.3264	−9.897	−0.0742	−4.924
Lan	21.111	27.481	21.723	9.161	1.2276	3.295	3.3776	16.538	0.3573	3.748
Pop	−0.0026	−2.617			0.0140	2.169	0.0131	50.391	0.0026	21.168
Pop_{s-1}	−0.0015	−2.544	−0.0014	−3.107	−0.0011	−3.998	−0.0012	−7.536		
Inc					−0.0036	−3.456				
Inc_{s-1}	−0.0356	−2.800	−0.0332	−2.458			−0.0141	−3.259		
Emr	−2342.5	−1.988	−2944.3	−3.562						
Emr_{s-1}					168.83	2.900	598.70	2.873		
Unr_{s-1}			−1844.4	−2.429						
Her	5165.5	4.002	5800.7	3.829						
Her_{s-1}					321.81	2.868	1166.1	2.674		
Ser					−119.87	−2.564				

(*continued on next page*)

Table 1 (*continued*).

Method	OLS		OLS-HAC		LAD		R-Winsorized		R-Bisquare	
x_l	β_l	z_l	β_l	z_l	β_l	z_l	β_l	z_l	β_l	z_l
Ser_{s-1}			−1500.6	−2.054	−215.10	−3.867	−699.82	−2.785		
Csr			3280.8	2.679						
Csr_{s-1}	5115.7	4.366	4673.1	4.049						
Cwr	4081.1	2.983	3385.2	3.444	327.27	5.126	802.67	3.479	258.76	4.072
Flu	3218.8	2.031	3402.0	2.195	377.24	3.060	908.53	2.250		
$R06_{s-1}$	−2175.4	−1.999	−1915.0	−2.040						
σ_e	2858.34		2897.84		3141.9		757.9[a]		360.21[a]	
R^2	0.420		0.404		0.344[b]		0.570[c]		0.584[c]	
-log(LF)	72849.26		72955.9		65978.51		.		.	
m	18		18		17		19		9	
Chi2[d]	5219.9		4684.4							
Chi2[e]	15802.4		12641.0		130909					

[a]Robust σ_e.
[b]Pseudo $R^2 = 1 - LF_m/LF_0$.
[c]Squared robust corr.$(y, \hat{y})$.
[d]Heteroskedasticity test.
[e]Normality test.

Table 2. Parameter estimates of the model of Eq. (4), dependent: y_{norm}, at $t = 2011$ (z_l are t-statistics).

Method	OLS		OLS-HAC		LAD		R-Winsorized		R-Bisquare	
x_l	β_l	z_l	β_l	z_l	β_l	z_l	β_l	z_l	β_l	z_l
Const.	0.7232	9.646	0.8346	7.787	0.0022	0.177	0.0281	2.008	−0.0111	−1.023
$y_{s,t-1}$	0.0303	2.558					0.4003	162.180	0.4294	213.560
$y_{s,t-2}$	0.5021	7.564			0.7145	2.273	0.2903	20.993	0.2172	19.300
$y_{s,t-3}$	1.3701	5.403	1.4399	3.913	1.4868	4.974	1.1327	21.446	0.8771	20.392
$y_{s,t-4}$									0.3311	2.679
$y_{s-1,t}$	0.1451	11.351	0.1543	4.515	0.0796	5.552	0.0713	27.128		
$y_{s-1,t-1}$	0.0179	2.088					0.0342	19.217	0.0362	24.971
$y_{s-1,t-2}$	0.1842	2.422								
Elv	−0.0002	−4.770	−0.0001	−4.249	−0.0001	−12.350	−0.0001	−10.136	−4.3E−05	−7.933
Lan					0.0002	7.476	0.0003	8.291	0.0002	7.268
Inc	−2.2E−05	−5.984	−2.4E−05	−7.556	−2.8E−06	−5.660	−5.2E−06	−6.601	−1.7E−06	−2.909
Inc_{s-1}					−1.8E−06	−3.487				
Emr					0.1473	3.339	0.2387	3.734		
Emr_{s-1}					0.0957	4.021			0.1185	3.681
Unr					−0.0347	−1.793				
Her_{s-1}					0.1510	3.568				
Ser	−0.8764	−3.859	−0.9035	−3.286	−0.1057	−3.528	−0.1645	−3.490		
Ser_{s-1}					−0.0905	−3.085			−0.0790	−2.224
Csr	−1.4924	−4.637	−1.8322	−4.489						
Cwr	1.0660	5.531	1.0517	5.246	0.1748	4.057	0.1873	2.474	0.1672	4.104
Flu	1.1098	2.770	1.1488	2.847	0.1986	3.835	0.3323	3.884		

(*continued on next page*)

autocorrelation consistent (HAC) standard errors [52]. The issue with OLS lies in the great number of large outliers (Fig. 7), which make the parameter estimates β_l and their t-statistics z_l biased and, therefore, unreliable. The typical diagnostic check is the analysis of residuals with respect to their 99.9% Gaussian acceptance region: $\left|\hat{e}_{st}\right| < 3\hat{\sigma}_e$ (Fig. 7, bottom panel). Dropping anomalous data or replacing them with OLS fitted values $\hat{y}_{st}$ is the usual remedy. However, the serial nature of observations prevents this approach from being applicable. In addition, a large amount of data (way more than 10%) should be repeatedly removed. Because of all the reasons above, we resort to the robust estimator of Eqs. (5)–(6), which has the advantage of keeping unchanged the dataset. Looking at the results, one may notice that the OLS method inflates the number of significant regressors but underestimates the global

Table 2 (*continued*).

Method	OLS		OLS-HAC		LAD		R-Winsorized		R-Bisquare	
x_l	β_l	z_l	β_l	z_l	β_l	z_l	β_l	z_l	β_l	z_l
Rbd			−0.0782	−3.096						
Rbd_{s-1}	−0.0839	−3.177	−0.0700	−4.254	−0.0105	−3.083	−0.0147	−2.783		
R81					0.0179	2.439			0.0297	2.716
σ_e	0.750		0.754		0.775		0.156[a]		0.127[a]	
R^2	0.054		0.046		0.286[b]		0.234[c]		0.207[c]	
-log(LF)	8786.08		8822.35		1296.64					
m	13		10		17		13		13	
Chi2[d]	142.140	(p0.0080)	112.490	(p0.0002)						
Chi2[e]	172579.0		173233.0		181562.0					

[a]Robust σ_e.
[b]Pseudo $R^2 = 1$ - LF_m/LF_0.
[c]Squared robust corr.$(y, \hat{y})$.
[d]Heteroskedasticity test.
[e]Normality test.

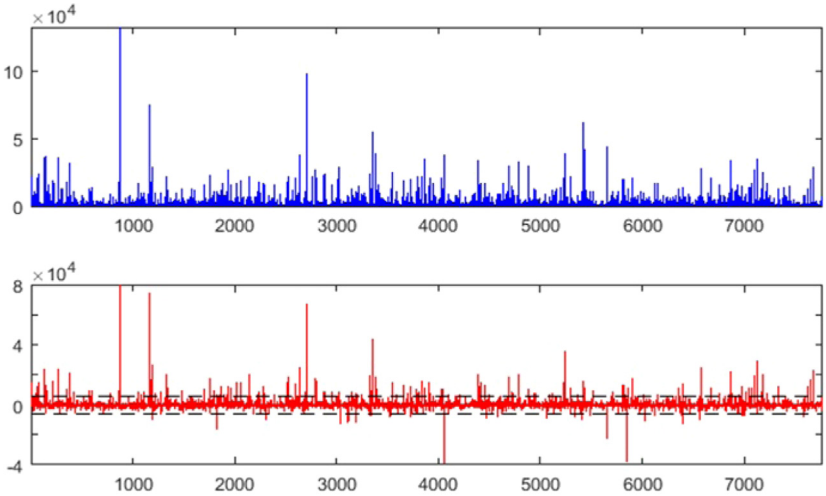

Fig. 7. Installed PV capacity data (top panel) and residuals of the OLS estimation for the model of Eq. (4) (bottom panel).

fitting performance. Both these features are clear symptoms of bias. Instead, the robust estimations substantially reduce the number of explanatory variables and make them consistent with the value of the R^2 index computed with Eq. (8).

Most of the time and space lags are significant and take on a positive sign, confirming that serial and spatial dependence occurs in the analyzed data. The time-dynamic component is of strong significance in shaping the installed PV capacity – also, as expected, the strength of that relationship decreases as time increases – whereas the spatial dynamic is not that important. However, both the overall and normalized installed PV capacity is positively affected by the simultaneous ($y_{s-1,t}$) and antecedent ($y_{s-1,t-1}$) PV adoption in the surrounding, confirming that peer effects and neighborhood effects are likely to affect the phenomenon under study.

As was anticipated, physical factors do matter, especially elevation with a negative sign and land area with a positive one. Most remarkable is that latitude is not a significant predictor of both overall and normalized installed PV capacity. One could argue that changing the slope of the panels lessens the constraint represented by the geographical location. Even so, there is a significant difference in the hours of sunlight between northern and southern Italy, especially during wintertime. Hence, it seems plausible to conclude that the subsidies provided with the support schemes have effectively sustained the adoption of PV systems in the less suitable areas. There are weak signs that the built environment (percentage of residential buildings built after 1981) is somehow related to the installed PV capacity.

Demography is an important driver since population turns out to be the most significant exogenous predictor of the overall installed PV capacity. Just a few findings are worth noting concerning the other socio-economic covariates. There is likely an inverse relationship between the disposable income per capita and the total installed PV capacity, and there is definitely an inverse relationship as far as the installed PV capacity normalized by population is concerned. Although the actual effect of income on PV is highly debated and a majority of studies found it positive, the opposite result we find in our case study could signal that public subsidies have been effective in supporting PV adoption in less wealthy areas. Finally, it deserves mentioning that the share of commuter workers in the population is positively related to the total and normalized installed PV capacity, and the spatial lags of a few predictors (employment rate, secondary- and higher education rate) are too. We believe that it is a further sign of spatial spillovers, which reinforce the conclusion that peer and neighborhood effects are significant in shaping the choices about PV energy.

5.2. Results for the global model

As a final analysis, we consider the space–time model of Eq. (3) with first-order lags $t-1, s-1$. According to the description in Section 3.2., its estimation is performed as in panel data models, namely, by stacking the time series of the spatial units and treating the time-invariant exogenous regressors as fixed-effects of the spatial units. Once again, the OLS estimates are meaningless due to massive outliers; they are hence omitted, and the robust approach of Eqs. (5)–(7) is applied. The tables below report the results concerning total (y_{oa}, Table 3) and normalized by population (y_{norm}, Table 4) installed PV capacity, respectively.

Table 3. Parameter estimates of the model in Eq. (3), dependent: y_{oa} (z_l are t-statistics).

Method	R-Winsorized		R-Bisquare	
x_l	β_l	z_l	β_l	z_l
Const.	−8.923100	−3.640	−0.443000	−0.304
$y_{s,t-1}$	1.403600	2510.9	1.008900	2644.8
$y_{s-1,t}$	0.058016	239.77	0.005187	31.263
$y_{s-1,t-1}$	0.040089	70.674	0.040462	103.84
Elv	−0.008135	−5.037		
Lan	0.092531	9.461		
Pop	0.000989	82.486	0.000385	51.243
Pop_{s-1}	−0.000211	−28.253	−0.000024	−4.726
Cwr	35.333000	4.792	9.522800	2.112
Flu	43.238000	2.144		
σ_e	86.39[a]		59.36[a]	
R^2	0.636[b]		0.633[b]	

[a]Robust σ_e.
[b]Squared robust correlation $(y, \hat{y})$.

Both the robust estimation functions – winsorized and bisquare – yield parsimonious results, with just a few significant predictors. Space and time lags do strongly matter, and the time trend outweighs the spatial dynamic. The global, panel-like model confirms the role played by physical factors, except for latitude, in facilitating – see the positive sign of the municipal land area – or in limiting – see the negative sign of elevation — the adoption of PV systems. We get further evidence that the overall installed PV capacity is strongly tied to population and, less markedly, to the share of commuter workers in the population, which can be interpreted as a confirmation that spatial spillovers occur. Besides, the normalized installed PV capacity is related to the employment rate, and there are weak signals of positive relationships with income and the percentage of commuter students.

Models in Tables 1–4 were built as in classical multiple regression, by inserting endogenous and exogenous regressors together and then by sequential elimination of 95% non-significant terms. To evaluate how much the exogenous variables X_{ls}, are actually correlated with the PV capacity Y_{st}, one can first regress it on its lagged

Table 4. Parameter estimates of the model in Eq. (3), dependent: y_{norm} (z_l are t-statistics).

Method	R-Winsorized		R-Bisquare	
x_l	β_l	z_l	β_l	z_l
Const.	−0.0044269	−5.195	0.0003838	0.755
$y_{s,t-1}$	0.5729900	1697.2	0.2778500	1015.8
$y_{s-1,t}$	0.1056400	524.54	0.0419880	257.39
$y_{s-1,t-1}$	0.0389920	158.23	0.0472360	236.61
Elv	−0.0000020	−4.857		
Lan	0.0000138	6.218	0.0000060	3.364
Inc			0.0000001	3.732
Emr	0.0145420	9.894		
Csr	0.0137800	3.496		
Rbd			−0.0011018	−3.782
σ_e	0.02183[a]		0.01767[a]	
R^2	0.460[b]		0.458[b]	

[a]Robust σ_e.

[b]Squared robust correlation $(y, \hat{y})$.

terms $Y_{s-j,t-i}$ and then its "residual" y_{st} (say) on the variables X_{ls} — all of these are performed with the robust estimators (5)–(6). The correlation $R(y_{st}, \hat{y}_{st})$, where $\hat{y}_{st}$ is the fitted value of the second regression, provides the partial correlation and is estimated with the robust formula (8). In our case study, it ranges from +0.27 to +0.36, depending on the various classes of models; in any event, they are all 99% significant with the classical F-statistic.

6. Conclusions

Modeling the phenomenon of solar PV deployment is truly challenging. It requires taking into account both the trend over time and across space; hence, the adoption of suitable space–time models is warranted. Besides, controlling for outliers is a major issue when dealing with big data; thus, employing robust estimation methods is inescapable. This study adopts robust estimation methods and space–time models to analyze the deployment of solar PV systems in Italy. Building on highly granular data, we use 7,797 observations of the installed PV capacity on a municipal basis and focus on the time window 2006–2011. The specificity of our approach lies in the fact that we model the spatial dynamic according to the notion of the nearest northwestern neighbor (NNWN). This means that we neither consider the nearest neighbor (NN) nor the k-nearest neighbors (k-NN) within a given radius, namely, the whole ring surrounding each municipality as usual in spatial autoregressive models. Instead, we impose a kind of identifiability constraint by limiting the spatial dependence relationship to the northwestern quadrant of each observation. That being so, the spatial dynamic is made unidirectional, just as the time dynamic is.

We show that serial and spatial dependence is an inherent characteristic of the analyzed data. The time-dynamic component is found to be more important than the spatial dynamic, and the strength of the relationship decreases as time increases. Regardless, the space lags are significant, which implies the occurrence of peer effects and neighborhood effects. Once serial and spatial dependence is properly taken into account, exogenous covariates narrow down to just a few physical (land area and elevation), demographic (population), and socio-economic drivers (mainly employment and commuting). Finally, it is worth noting that we found a mostly negative relationship between the installed PV capacity and income and no relationship with latitude. We interpret this as a signal of the effectiveness of the support schemes and the related subsidies in incentivizing the adoption of solar PV systems in less wealthy and less suitable areas of the country.

Declaration of competing interest

The authors declare that they have no known competing financial interests or personal relationships that could have appeared to influence the work reported in this paper.

Appendix. On *triangular* contiguity matrices

To briefly show the statistical issues that the misspecification of the spatial lag structure of the model in Eq. (2) creates, let us consider a simple SAR model in matrix version of Eq. (3), namely, $\boldsymbol{y} = \varphi \boldsymbol{W}\boldsymbol{y} + \boldsymbol{e}$ with $\boldsymbol{e} \sim \mathrm{N}(0, \boldsymbol{I}_n \sigma_e^2)$ independent and $\boldsymbol{W}$ the contiguity matrix. Notice that the model can be rewritten in *reduced* form as $\boldsymbol{y} = (\boldsymbol{I}_n - \varphi \boldsymbol{W})^{-1}\boldsymbol{e}$ and this shows a first issue about the conditions of invertibility of the response matrix. By letting $\boldsymbol{x} = \boldsymbol{W}\boldsymbol{y}$, the ordinary least squares (OLS) estimator of φ is given by $\hat{\varphi}_n = (\boldsymbol{x}'\boldsymbol{x})^{-1}\boldsymbol{x}'\boldsymbol{y} = \varphi + (\boldsymbol{x}'\boldsymbol{x})^{-1}\boldsymbol{x}'\boldsymbol{e}$, and its unbiasedness $\mathrm{E}\left(\hat{\varphi}_n\right) = \varphi$ holds only if the expectation $\mathrm{E}\left(\boldsymbol{x}'\boldsymbol{e}\right) = 0$. Now, from previous expressions we have $\mathrm{E}\left(\boldsymbol{x}'\boldsymbol{e}\right) = \mathrm{E}[\boldsymbol{e}'(\boldsymbol{I}_n - \varphi \boldsymbol{W}')^{-1}\boldsymbol{W}'\boldsymbol{e}]$, which is 0 only if the trace (tr) of the matrix $\boldsymbol{G}' = (\boldsymbol{I}_n - \varphi \boldsymbol{W}')^{-1}\boldsymbol{W}'$ is 0; in fact, $\mathrm{E}\left(\boldsymbol{x}'\boldsymbol{e}\right) = \mathrm{E}\left[\mathrm{tr}\left(\boldsymbol{e}'\boldsymbol{G}'\boldsymbol{e}\right)\right] = \mathrm{tr}\left[\boldsymbol{G}\mathrm{E}\left(\boldsymbol{e}\boldsymbol{e}'\right)\right]$.

In the spatial econometric literature, the weights matrix $\boldsymbol{W}$ is usually based on *circular* neighbors (e.g. of *rook* or *queen* type); these involve $\mathrm{tr}(\boldsymbol{G}) \neq 0$ and thus the inconsistency of OLS method. To address this issue, alternative estimators have been proposed, such as maximum likelihood (ML) [45], generalized method of moments (GMM) [41], and indirect inference (II) [7]. However, under regularity conditions, OLS enjoys optimal properties and by constraining $\boldsymbol{W}$ to a single spatial direction, its optimality is preserved. In the lattice literature [31], unidirectionality is the favorite constraint, the more severe of which is the *one-quadrant* specification: $y_{ij} = \varphi y_{i-k,j-h} + e_{ij}$, with $k, h = 0, 1$. As in standard time series, this allows recursive forecasting and causal decomposition in the moving average form $y_{ij} = \sum_{k=0}^{\infty}\sum_{h=0}^{\infty}\varphi^{k+h}e_{i-k,j-h}$.

Using the vector notation $\boldsymbol{y} = \varphi \boldsymbol{W}\boldsymbol{y} + \boldsymbol{e}$, one can also show that the *full* one-quadrant model $y_{ij} = \varphi(y_{i,j-1} + y_{i-1,j-1} + y_{i-1,j})/3 + e_{ij}$ involves a lower triangular matrix $\boldsymbol{W}$, with 1/3 in the three lower sub-diagonals. The *triangularity* of $\boldsymbol{W}$ is also retained in the areal data model $y_s = \varphi y_{s-1} + e_s$, provided that the observations y_s in the vector $\boldsymbol{y}$ are sorted by the distance from the upper-left corner. In practice, if $\boldsymbol{l}_s = (i_s, j_s)$ are the spatial coordinates of observations y_s and $\mathrm{D}(.)$ is the Euclidean distance, then the ordering in the vector $\boldsymbol{y}$ must be such that $\mathrm{D}(\boldsymbol{l}_{s-1}, \boldsymbol{l}_0) \leq \mathrm{D}(\boldsymbol{l}_s, \boldsymbol{l}_0)$ for all s, where $\boldsymbol{l}_0$ is the upper-left corner. In these conditions, the response matrix $(\boldsymbol{I}_n - \varphi \boldsymbol{W})^{-1}$ is always invertible and $\mathrm{tr}(\boldsymbol{G}) = 0$; in particular, each component y_s of $\boldsymbol{y}$ can be expressed as a function of e_{s-k}, $k > 0$ only, and $\mathrm{E}\left[(\boldsymbol{W}\boldsymbol{y})'\boldsymbol{e}\right] = 0$. Notice that these properties *do not* hold in the case the terms $y_{s-1} = \boldsymbol{W}\boldsymbol{y}$ are just defined as the nearest neighbors of y_s and/or y_s are not ordered.

Previous results can be extended to more complex systems with exogenous regressors and space–time dynamics. For the STARX system (2), we carry out simulation experiments to show the consistency of OLS in the presence of unidirectional specification of the matrix $\boldsymbol{W}$. In particular, for the model (1), with single regressor $x_t \sim \mathrm{U}(0, 1)$ and coefficients $\alpha = 1$, $\beta_1 = 2, \beta_2 = -1, \varphi_1 = 0.6, \varphi_2 = 0.5, \varphi_3 = -0.5, \sigma_e = 1$, we generate $n = 100$ random spatial points $i_s, j_s \sim \mathrm{U}(0, 1)$ and $T = 100$ time periods. With these coordinates, we built the matrices $\boldsymbol{W}_{1,2}$ of simple (circular) NN and upper-left NN (Fig. A.1), and generate the data with the model (3) written in reduced form:

$$\boldsymbol{y}_t = (\boldsymbol{I}_n - \varphi_2 \boldsymbol{W})^{-1}\left[\alpha \mathbf{1}_n + (\varphi_1 + \varphi_3 \boldsymbol{W})\,\boldsymbol{y}_{t-1} + (\beta_1 + \boldsymbol{W}\beta_2)\,\boldsymbol{x}_t + \boldsymbol{e}_t\right] \tag{A.1}$$

Finally, we apply the OLS estimator $\hat{\boldsymbol{\delta}}_N = (\boldsymbol{Z}_N'\boldsymbol{Z}_N)^{-1}\boldsymbol{Z}_N'\boldsymbol{y}_N$, with $N = n \cdot T$, to the matrix $\boldsymbol{Z}_N$ composed by the stacked blocks $\boldsymbol{Z}_t = \left[\mathbf{1}_n, \boldsymbol{x}_t, \boldsymbol{W}\boldsymbol{x}_t, \boldsymbol{y}_{t-1}, \boldsymbol{W}\boldsymbol{y}_t, \boldsymbol{W}\boldsymbol{y}_{t-1}\right]$, as in panel models. We replicate the procedure $M = 1000$ times and we compute mean values and root mean squared errors: $\mathrm{RMSE}_j = [M^{-1}\sum_{i=1}^{M}(\hat{\delta}_{ij} - \delta_{ij})^2]^{1/2}$ of estimates, together with the p-values of normality test statistic of Jarque and Bera [38].

Table A.1. Results of simulation experiment on the model (1) estimated with OLS with matrix $\boldsymbol{W}_{\mathrm{NN}}$ (first block) and $\boldsymbol{W}_{\mathrm{NW}}$ (second block). Statistics are computed on $M = 1000$ replications.

	α_0 (1)	β_1 (2)	β_2 (−1)	φ_1 (0.6)	φ_2 (0.5)	φ_3 (−0.5)
Mean	0.6015	1.9709	−1.3752	0.7662	0.5369	−0.5424
RMSE	0.3994	0.0439	0.3768	0.1663	0.0376	0.0430
N-test	0.3002	0.9352	0.4759	0.5835	0.9097	0.1774
Mean	0.9988	2.0000	−0.9984	0.5999	0.5000	−0.4998
RMSE	0.0394	0.0347	0.0369	0.0074	0.0068	0.0079
N-test	0.4184	0.1809	0.3924	0.1427	0.1441	0.8721

The results are reported in Table A.1; they show a significant better performance of OLS in the model with one-quadrant $\boldsymbol{W}_{\mathrm{NW}}$, with respect to the simple NN contiguity. The simulation experiment is extended to data

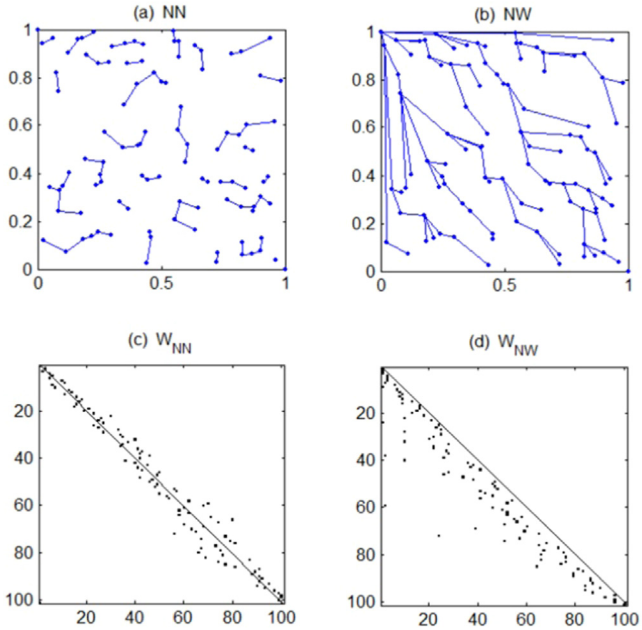

Fig. A.1. Plot of $n = 100$ spatial points $i_s, j_s \sim \mathrm{U}(0, 1)$, and their NN and NW connections (a,b); Corresponding spatial weights matrices $\boldsymbol{W}$ (where NW is triangular) (c,d).

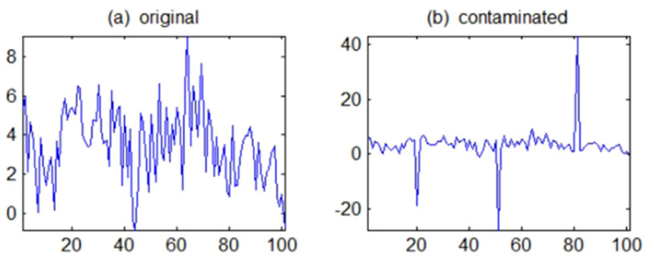

Fig. A.2. A sample realization $\boldsymbol{y}_t$ of the model in Eq. (A.1) and its contamination with outliers $y^*_{st} = 30, -70, 50$ placed at random locations $s^* \sim \mathrm{U}(1, n)$ at each t.

Table A.2. Results as in Table A.1, but computed on series contaminated as in Fig. A.2 and $M = 100$ replications.

	α_0 (1)	β_1 (2)	β_2 (−1)	φ_1 (0.6)	φ_2 (0.5)	φ_3 (−0.5)
Mean	2.0601	2.0181	0.1259	0.0693	0.3931	−0.3005
RMSE	1.0775	0.3264	1.1651	0.5309	0.1074	0.1998
N-test	0.6356	0.6148	0.6902	0.8730	0.5236	0.0000
Mean	1.5519	1.9220	0.0508	0.0737	0.4881	−0.2372
RMSE	0.6047	0.3341	1.1058	0.5268	0.0149	0.2636
N-test	0.8151	0.8269	0.3645	0.1262	0.9358	0.1848

contaminated by outliers and to the robust estimators (5)–(6). The data $\boldsymbol{y}_t$ of the model are contaminated with three fixed outliers $y^*_{st} = 30, -70, 50$, placed at random locations $s^* \sim \mathrm{U}(1, n)$ for each t (Fig. A.2); these outliers heavily bias the OLS estimates for both $\boldsymbol{W}$ matrices (Table A.2). Instead, the results of robust estimates (5)–(6) with tuning constant $\gamma = 2$ and $M = 100$ replications are displayed in Table A.3; they show a satisfactory performance, especially with the matrix $\boldsymbol{W}_{\mathrm{NW}}$. Hence, the one-quadrant constraint does also work with general estimators; these

Table A.3. Results as in Table A.2, but provided by the robust estimator (5)-(6) with tuning constant $\gamma = 2$.

	α_0 (1)	β_1 (2)	β_2 (−1)	φ_1 (0.6)	φ_2 (0.5)	φ_3 (−0.5)
Mean	0.8725	1.9788	−1.1417	0.6686	0.5125	−0.5249
RMSE	0.1343	0.0613	0.1525	0.0693	0.0129	0.0252
N-test	0.7923	0.9103	0.3008	0.4035	0.1915	0.1431
Mean	0.9987	2.0056	−1.0050	0.6013	0.5000	−0.5007
RMSE	0.0357	0.0418	0.0547	0.0043	0.0012	0.0026
N-test	0.6156	0.6480	0.2421	0.0123	0.5070	0.1132

results fully legitimate the use of OLS and robust estimators with $\boldsymbol{W}_{\mathrm{NW}}$ matrix in complex real situations, such as PV deployment.

References

[1] Abreu J, Wingartz N, Hardy N. New trends in solar: A comparative study assessing the attitudes towards the adoption of rooftop PV. Energy Policy 2019;128:347–63. http://dx.doi.org/10.1016/j.enpol.2018.12.038.
[2] Alipour M, Salim H, Stewart RA, Sahin O. Predictors, taxonomy of predictors, and correlations of predictors with the decision behaviour of residential solar photovoltaics adoption: A review. Renew. Sustain. Energy Rev. 2020;123:109749. http://dx.doi.org/10.1016/j.rser.2020.109749.
[3] Allan GJ, McIntyre SG. Green in the heart or greens in the wallet? The spatial uptake of small-scale renewable technologies. Energy Policy 2017;102:108–15. http://dx.doi.org/10.1016/j.enpol.2016.12.005.
[4] Andrews DWK. Heteroskedasticity and autocorrelation consistent covariance matrix estimation. Econometrica 1991;59:817–58. http://dx.doi.org/10.2307/2938229.
[5] Balta-Ozkan N, Yildirim J, Connor PM. Regional distribution of photovoltaic deployment in the UK and its determinants: A spatial econometric approach. Energy Econ. 2015;51:417–29. http://dx.doi.org/10.1016/j.eneco.2015.08.003.
[6] Balta-Ozkan N, Yildirim J, Connor PM, Truckell I, Hart P. Energy transition at local level: Analyzing the role of peer effects and socio-economic factors on UK solar photovoltaic deployment. Energy Policy 2021;148:112004. http://dx.doi.org/10.1016/j.enpol.2020.112004.
[7] Bao Y, Liu X, Yang L. Indirect inference estimation of spatial autoregressions. Econometrics 2020;8(34). http://dx.doi.org/10.3390/econometrics8030034.
[8] Bashiri A, Alizadeh SH. The analysis of demographics, environmental and knowledge factors affecting prospective residential PV system adoption: A study in Tehran. Renew. Sustain. Energy Rev. 2018;81:3131–9. http://dx.doi.org/10.1016/j.rser.2017.08.093.
[9] Bollinger B, Gillingham K. Peer effects in the diffusion of solar photovoltaic panels. Mark. Sci. 2012;31:900–12. http://dx.doi.org/10.1287/mksc.1120.0727.
[10] Bondio S, Shahnazari M, McHugh A. The technology of the middle class: Understanding the fulfilment of adoption intentions in Queensland's rapid uptake residential solar photovoltaics market. Renew. Sustain. Energy Rev. 2018;93:642–51. http://dx.doi.org/10.1016/j.rser.2018.05.035.
[11] Braito M, Flint C, Muhar A, Penker M, Vogel S. Individual and collective socio-psychological patterns of photovoltaic investment under diverging policy regimes of Austria and Italy. Energy Policy 2017;109:141–53. http://dx.doi.org/10.1016/j.enpol.2017.06.063.
[12] Bramati MC. Robust Lavalle'e-Hidiroglou stratified sampling strategy. Surv. Res. Methods 2012;6:137–43. http://dx.doi.org/10.18148/SRM/2012.V6I3.5130.
[13] Bustos O, Ojeda S, Vallejos R. Spatial ARMA models and its applications to image filtering. Braz. J. Probab. Stat. 2009;23:141–65. http://dx.doi.org/10.1214/08-BJPS019.
[14] Carfora A, Romano AA, Ronghi M, Scandurra G. Renewable generation across Italian regions: Spillover effects and effectiveness of European Regional Fund. Energy Policy 2017;102:132–41. http://dx.doi.org/10.1016/j.enpol.2016.12.027.
[15] Comello S, Reichelstein S, Sahoo A. The road ahead for solar PV power. Renew. Sustain. Energy Rev. 2018;92:744–56. http://dx.doi.org/10.1016/j.rser.2018.04.098.
[16] Copiello S. Building energy efficiency: A research branch made of paradoxes. Renew. Sustain. Energy Rev. 2017;69:1064–76. http://dx.doi.org/10.1016/j.rser.2016.09.094.
[17] Copiello S, Grillenzoni C. Solar photovoltaic energy and its spatial dependence. Energy Procedia 2017;141:86–90. http://dx.doi.org/10.1016/j.egypro.2017.11.017.
[18] Copiello S, Grillenzoni C. Economic development and climate change. Which is the cause and which the effect? Energy Rep. 2020;6:49–59. http://dx.doi.org/10.1016/j.egyr.2020.08.024.
[19] Curtius HC, Hille SL, Berger C, Hahnel UJJ, Wüstenhagen R. Shotgun or snowball approach? Accelerating the diffusion of rooftop solar photovoltaics through peer effects and social norms. Energy Policy 2018;118:596–602. http://dx.doi.org/10.1016/j.enpol.2018.04.005.
[20] De Groote O, Pepermans G, Verboven F. Heterogeneity in the adoption of photovoltaic systems in Flanders. Energy Econ. 2016;59:45–57. http://dx.doi.org/10.1016/j.eneco.2016.07.008.
[21] Dharshing S. Household dynamics of technology adoption: A spatial econometric analysis of residential solar photovoltaic (PV) systems in Germany. Energy Res. & Soc. Sci. 2017;23:113–24. http://dx.doi.org/10.1016/j.erss.2016.10.012.

[22] Dietz RD. The estimation of neighborhood effects in the social sciences: An interdisciplinary approach q. Soc. Sci. Res. 2002;31:539–75. http://dx.doi.org/10.1016/S0049-089X(02)00005-4.
[23] Ding H, Zhou DQ, Liu GQ, Zhou P. Cost reduction or electricity penetration: Government R & D-induced PV development and future policy schemes. Renew. Sustain. Energy Rev. 2020;124:109752. http://dx.doi.org/10.1016/j.rser.2020.109752.
[24] Dusonchet L, Telaretti E. Economic analysis of different supporting policies for the production of electrical energy by solar photovoltaics in western European Union countries. Energy Policy 2010;38:3297–308. http://dx.doi.org/10.1016/j.enpol.2010.01.053.
[25] Elhorst JP. Spatial Econometrics, SpringerBriefs in Regional Science. Berlin, Heidelberg: Springer Berlin Heidelberg; 2014, http://dx.doi.org/10.1007/978-3-642-40340-8.
[26] Escoffier M, Hache E, Mignon V, Paris A. Determinants of solar photovoltaic deployment in the electricity mix: Do oil prices really matter? Energy Economics 2020;105024. http://dx.doi.org/10.1016/j.eneco.2020.105024.
[27] Eshraghi J, Narjabadifam N, Mirkhani N, Sadoughi Khosroshahi S, Ashjaee M. A comprehensive feasibility study of applying solar energy to design a zero energy building for a typical home in Tehran. Energy Build. 2014;72:329–39. http://dx.doi.org/10.1016/j.enbuild.2014.01.001.
[28] European Commission. A Clean Planet for all - A European strategic long-term vision for a prosperous, modern, competitive and climate neutral economy. Brussels, 2018.
[29] European Commission. The European Green Deal. Brussels, 2019.
[30] Graziano M, Gillingham K. Spatial patterns of solar photovoltaic system adoption: The influence of neighbors and the built environment. J. Econ. Geogr. 2015;15:815–39. http://dx.doi.org/10.1093/jeg/lbu036.
[31] Grillenzoni C. Adaptive spatio-temporal models for satellite ecological data. JABES 2004;9:158–80. http://dx.doi.org/10.1198/1085711043541.
[32] Grillenzoni C. Design of kernel M-smoothers for spatial data. Stat. Methodol. 2008;5:220–37. http://dx.doi.org/10.1016/j.stamet.2007.08.003.
[33] Haines A, Scheelbeek P. European Green deal: a major opportunity for health improvement. Lancet 2020;395:1327–9. http://dx.doi.org/10.1016/S0140-6736(20)30109-4.
[34] Hansen K, Breyer C, Lund H. Status and perspectives on 100% renewable energy systems. Energy 2019;175:471–80. http://dx.doi.org/10.1016/j.energy.2019.03.092.
[35] Jäger-Waldau A. Snapshot of photovoltaics - february 2018. EPJ Photovolt 2018;9:6. http://dx.doi.org/10.1051/epjpv/2018004.
[36] Jäger-Waldau A, Kakoulaki G, Kougias I, Taylor N. The European green deal - what's in it for photovoltaics?. In: 2020 47th IEEE Photovoltaic Specialists Conference (PVSC). Presented At the 2020 IEEE 47th Photovoltaic Specialists Conference (PVSC). Calgary, OR: IEEE; 2020a, p. 0927–31. http://dx.doi.org/10.1109/PVSC45281.2020.9300767.
[37] Jäger-Waldau A, Kougias I, Taylor N, Thiel C. How photovoltaics can contribute to GHG emission reductions of 55% in the EU by 2030. Renew. Sustain. Energy Rev. 2020b;126:109836. http://dx.doi.org/10.1016/j.rser.2020.109836.
[38] Jarque CM, Bera AK. A test for normality of observations and regression residuals. Int. Stat. Rev. / Revue Int. de Stat. 1987;55:163. http://dx.doi.org/10.2307/1403192.
[39] Karakaya E, Hidalgo A, Nuur C. Motivators for adoption of photovoltaic systems at grid parity: A case study from Southern Germany. Renew. Sustain. Energy Rev. 2015;43:1090–8. http://dx.doi.org/10.1016/j.rser.2014.11.077.
[40] Kavlak G, McNerney J, Trancik JE. Evaluating the causes of cost reduction in photovoltaic modules. Energy Policy 2018;123:700–10. http://dx.doi.org/10.1016/j.enpol.2018.08.015.
[41] Kelejian HH, Prucha IR. Specification and estimation of spatial autoregressive models with autoregressive and heteroskedastic disturbances. J. Econometrics 2010;157:53–67. http://dx.doi.org/10.1016/j.jeconom.2009.10.025.
[42] Korcaj L, Hahnel UJJ, Spada H. Intentions to adopt photovoltaic systems depend on homeowners' expected personal gains and behavior of peers. Renew. Energy 2015;75:407–15. http://dx.doi.org/10.1016/j.renene.2014.10.007.
[43] Kosugi T, Shimoda Y, Tashiro T. Neighborhood influences on the diffusion of residential photovoltaic systems in Kyoto City, Japan. Environ. Econ. Policy Stud. 2019;21:477–505. http://dx.doi.org/10.1007/s10018-019-00239-5.
[44] Kwan CL. Influence of local environmental, social, economic and political variables on the spatial distribution of residential solar PV arrays across the United States. Energy Policy 2012;47:332–44. http://dx.doi.org/10.1016/j.enpol.2012.04.074.
[45] LeSage JP, Pace RK. Introduction To Spatial Econometrics. Boca Raton: CRC Press; 2009.
[46] Maronna RA, Douglas Martin R, Yohai VJ, Salibián-Barrera M. Robust Statistics: Theory and Methods. second ed.. Hoboken: John Wiley & Sons; 2018.
[47] Müller S, Rode J. The adoption of photovoltaic systems in Wiesbaden, Germany. Econ. Innov. New Technol. 2013;22:519–35. http://dx.doi.org/10.1080/10438599.2013.804333.
[48] Müller J, Trutnevyte E. Spatial projections of solar PV installations at subnational level: Accuracy testing of regression models. Appl. Energy 2020;265:114747. http://dx.doi.org/10.1016/j.apenergy.2020.114747.
[49] Mundaca L, Samahita M. What drives home solar PV uptake? Subsidies, peer effects and visibility in Sweden. Energy Res. & Soc. Sci. 2020;60:101319. http://dx.doi.org/10.1016/j.erss.2019.101319.
[50] Murakami T. Agent-based simulations of the influence of social policy and neighboring communication on the adoption of grid-connected photovoltaics. Energy Convers. Manage. 2014;80:158–64. http://dx.doi.org/10.1016/j.enconman.2014.01.033.
[51] Nemet GF. Beyond the learning curve: factors influencing cost reductions in photovoltaics. Energy Policy 2006;34:3218–32. http://dx.doi.org/10.1016/j.enpol.2005.06.020.
[52] Newey WK, West KD. A simple, positive semi-definite, heteroskedasticity and autocorrelation consistent covariance matrix. Econometrica 1987;55:703. http://dx.doi.org/10.2307/1913610.
[53] Noll D, Dawes C, Rai V. Solar community organizations and active peer effects in the adoption of residential PV. Energy Policy 2014;67:330–43. http://dx.doi.org/10.1016/j.enpol.2013.12.050.

[54] Orioli A, Di Gangi A. The recent change in the Italian policies for photovoltaics: Effects on the payback period and levelized cost of electricity of grid-connected photovoltaic systems installed in urban contexts. Energy 2015;93:1989–2005. http://dx.doi.org/10.1016/j.energy.2015.10.089.
[55] Orioli A, Di Gangi A. Six-years-long effects of the Italian policies for photovoltaics on the grid parity of grid-connected photovoltaic systems installed in urban contexts. Energy 2017;130:55–75. http://dx.doi.org/10.1016/j.energy.2017.04.069.
[56] Ortega-Izquierdo M, del Río P. Benefits and costs of renewable electricity in Europe. Renew. Sustain. Energy Rev. 2016;61:372–83. http://dx.doi.org/10.1016/j.rser.2016.03.044.
[57] Palm A. Local factors driving the diffusion of solar photovoltaics in Sweden: A case study of five municipalities in an early market. Energy Res. & Soc. Sci. 2016;14:1–12. http://dx.doi.org/10.1016/j.erss.2015.12.027.
[58] Palm A, Lantz B. Information dissemination and residential solar PV adoption rates: The effect of an information campaign in Sweden. Energy Policy 2020;142:111540. http://dx.doi.org/10.1016/j.enpol.2020.111540.
[59] Palmer J, Sorda G, Madlener R. Modeling the diffusion of residential photovoltaic systems in Italy: An agent-based simulation. Technol. Forecast. 2015;99:106–31. http://dx.doi.org/10.1016/j.techfore.2015.06.011.
[60] Pohoryles DA, Maduta C, Bournas DA, Kouris LA. Energy performance of existing residential buildings in Europe: A novel approach combining energy with seismic retrofitting. Energy Build. 2020;223:110024. http://dx.doi.org/10.1016/j.enbuild.2020.110024.
[61] Polo AL, Haas R. An international overview of promotion policies for grid-connected photovoltaic systems: An international overview of promotion policies. Prog. Photovolt: Res. Appl. 2014;22:248–73. http://dx.doi.org/10.1002/pip.2236.
[62] Rai V, Reeves DC, Margolis R. Overcoming barriers and uncertainties in the adoption of residential solar PV. Renew. Energy 2016;89:498–505. http://dx.doi.org/10.1016/j.renene.2015.11.080.
[63] Robinson SA, Rai V. Determinants of spatio-temporal patterns of energy technology adoption: An agent-based modeling approach. Appl. Energy 2015;151:273–84. http://dx.doi.org/10.1016/j.apenergy.2015.04.071.
[64] Rode J, Weber A. Does localized imitation drive technology adoption? A case study on rooftop photovoltaic systems in Germany. J. Environ. Econ. Manag. 2016;78:38–48. http://dx.doi.org/10.1016/j.jeem.2016.02.001.
[65] Sardianou E, Genoudi P. Which factors affect the willingness of consumers to adopt renewable energies? Renew. Energy 2013;57:1–4. http://dx.doi.org/10.1016/j.renene.2013.01.031.
[66] Schaffer AJ, Brun S. Beyond the sun—Socioeconomic drivers of the adoption of small-scale photovoltaic installations in Germany. Energy Res. & Soc. Sci. 2015;10:220–7. http://dx.doi.org/10.1016/j.erss.2015.06.010.
[67] Shevlyakov G, Smirnov P. Robust estimation of the correlation coefficient: An attempt of survey. Austrian J. Stat. 2011;40:147–56. http://dx.doi.org/10.17713/ajs.v40i1&2.206.
[68] Strazzera E, Statzu V. Fostering photovoltaic technologies in Mediterranean cities: Consumers' demand and social acceptance. Renew. Energy 2017;102:361–71. http://dx.doi.org/10.1016/j.renene.2016.10.056.
[69] ˇ Súri M, Huld TA, Dunlop ED, Ossenbrink HA. Potential of solar electricity generation in the European Union member states and candidate countries. Sol. Energy 2007;81:1295–305. http://dx.doi.org/10.1016/j.solener.2006.12.007.
[70] Szabó S, Bódis K, Kougias I, Moner-Girona M, Jäger-Waldau A, Barton G, Szabó L. A methodology for maximizing the benefits of solar landfills on closed sites. Renew. Sustain. Energy Rev. 2017;76:1291–300. http://dx.doi.org/10.1016/j.rser.2017.03.117.
[71] Tobler WR. A computer movie simulating urban growth in the detroit region. Econ. Geogr. 1970;46:234–40. http://dx.doi.org/10.2307/143141.
[72] Trancik JE, Cross-Call D. Energy technologies evaluated against climate targets using a cost and carbon trade-off curve. Environ. Sci. Technol. 2013;47:6673–80. http://dx.doi.org/10.1021/es304922v.
[73] Trippel E. How green is green enough? The changing landscape of financing a sustainable European economy. ERA Forum 2020;21:155–70. http://dx.doi.org/10.1007/s12027-020-00611-z.
[74] Van Aelst S, Willems G, Zamar RH. Robust and efficient estimation of the residual scale in linear regression. J. Multivariate Anal. 2013;116:278–96. http://dx.doi.org/10.1016/j.jmva.2012.12.008.
[75] Vartiainen E, Masson G, Breyer C, Moser D, Román Medina E. Impact of weighted average cost of capital, capital expenditure, and other parameters on future utility-scale PV levelised cost of electricity. Prog. Photovolt. Res. Appl. 2020;28:439–53. http://dx.doi.org/10.1002/pip.3189.
[76] Vasseur V, Kemp R. The adoption of PV in the netherlands: A statistical analysis of adoption factors. Renew. Sustain. Energy Rev. 2015;41:483–94. http://dx.doi.org/10.1016/j.rser.2014.08.020.
[77] Yamamoto Y. Opinion leadership and willingness to pay for residential photovoltaic systems. Energy Policy 2015;83:185–92. http://dx.doi.org/10.1016/j.enpol.2015.04.014.